

RESEARCH ARTICLE

ARTIFICIAL INFILTRATION MODEL TO INCREASE INFILTRATION CAPACITY IN URBAN RESIDENTIAL LAND

Totoh Andayono^{a,b}, Mas Mera^c, Junaidi^c, Dalrino^d, Riko Maiyudi^e, Aulia H Burhamidar^{e*}^aDoctor Student in Civil Engineering at University of Andalas, Indonesia^bCivil Engineering, Padang State University, Padang, Indonesia^cCivil Engineering, University of Andalas, Padang, Indonesia^dCivil Engineering, Padang State Polytechnics, Padang, Indonesia^eMining Engineering Department, Padang State University, Padang, Indonesia^{*}Corresponding Author Email: mas_mera@eng.unand.ac.id

This is an open access journal distributed under the Creative Commons Attribution License CC BY 4.0, which permits unrestricted use, distribution, and reproduction in any medium, provided the original work is properly cited

ARTICLE DETAILS

Article History:

Received 01 May 2024

Revised 03 June 2024

Accepted 06 July 2024

Available online 17 July 2024

ABSTRACT

The change of land use from rainwater catchment area to residential land has an effect on changes in soil parameters. These changes can reduce infiltration capacity. The aim of this research is to design an artificial infiltration model to increase infiltration capacity in urban residential land with the criteria: easy to make, economical, can be applied on limited area, does not disturb bearing capacity, and can be integrated with the urban drainage system. This new infiltration model considers the groundwater level, embankment thickness, and the ratio of yard area to house area. This artificial infiltration model is box-shaped with dimensions of 50cm x 50cm x 100cm, filled with split and a 4 inches perforated-PVC pipe installed in the center. The pipe is installed vertically, where the top of the pipe branches horizontally to drain off excess water into urban drainage. The soil parameters used in this model are the same as the soil in residential areas. The model results show that the infiltration capacity is 342 mm/hour. Meanwhile, the surface infiltration capacity measured using a double ring infiltrometer was 59mm/hour. Comparison of these results shows that the infiltration model is able to increase infiltration capacity up to 6 times. The model is also capable of slowing down initiation of surface runoff. Therefore, rainwater that falls on the ground surface can be absorbed quickly into the ground, which make surface runoff smaller.

KEYWORDS

Artificial infiltration, Infiltration capacity, Residential land

1. INTRODUCTION

Naturally, most of the rain that falls on the ground surface seeps into the soil through an infiltration process (Kuma et al., 2023; Mgolozeli et al., 2022). Infiltration is closely related to soil parameters, structure, texture, void distribution and water supply (Basset et al., 2023). The development of a city causes changes in land use, where rainwater catchment area changes into residential area, causing changes in soil parameters (Molla et al., 2022; Xiao et al., 2023; Basset et al., 2023; Locatelli et al., 2017). On residential land, subgrade soil is often replaced with low permeability and high bearing capacity landfill. Heavy equipment is used to compact embankment during construction activities, also resulting in changes in structure, texture, void distribution and water supply (Kodikara et al., 2018; Obour and Ugarte, 2021). Soil compaction causes changes in porosity, infiltration capacity and groundwater holding capacity, which resulting increase in value and an accelerate the occurrence of peak discharge (Alaoui et al., 2018; Andayono, 2018).

This condition can be overcome by increasing the infiltration capacity of the compacted soil (Arvand et al., 2023; Zaqout et al., 2022). The use of artificial infiltration could be one of the solutions (Shahzad et al., 2022). In practice, artificial infiltration is known as eco-drainage, which use to slow down the flow of runoff water into rivers in order to prevent flooding due to an increase in peak discharge. Various forms of eco-drainage that are widely applied are leaky wells, retention trenches, infiltration basins, infiltration cells, seepage pipes and rain water harvesting (Meng et al.,

2022; Wu et al., 2023). This artificial infiltration tool, substantively, water conservation by absorbing rainwater into the ground as a groundwater reserve which decreasing surface runoff (Bean and Dukes, 2015; Fahim Aslam et al., 2021; Jennings and Baker, 2016; Kirenda and Mugume, 2019; Yu et al., 2022).

The aim of this research is to create an artificial infiltration model that can be used in laboratory to increase infiltration capacity and reduce surface runoff. It is hoped that this model can later be well-developed and applied in residential areas.

2. MATERIAL AND METHODS

This research was carried out in several stages. The first stage was taking samples in the quarry. Quarry soil was used as a sample in testing the artificial infiltration model. These quarry soil samples came from 5 quarry locations which are usually used as landfill for settlements.

The second stage is direct measurements in the field to obtain the groundwater level, thickness of the embankment layer, the ratio of yard area to house building area for one plot, and infiltration data. Infiltration measurements in residential land were carried out in one of the residential areas in Kuranji District, Padang City, West Sumatra Province (Figure 1).

The third stage is testing samples in the laboratory to obtain soil parameters such as soil water content (ω), soil bulk density (γ), soil specific gravity (G_s), soil porosity (n), soil texture, dry soil bulk density (γ_d), field

Quick Response Code



Access this article online

Website:

www.watconman.org

DOI:

10.26480/wcm.04.2024.396.401

soil density, soil permeability, and strength. absorb split. The fourth stage is to design a new infiltration model based on conditions in the settlement,

namely groundwater level, average thickness of embankment, and ratio of yard area to house building area.

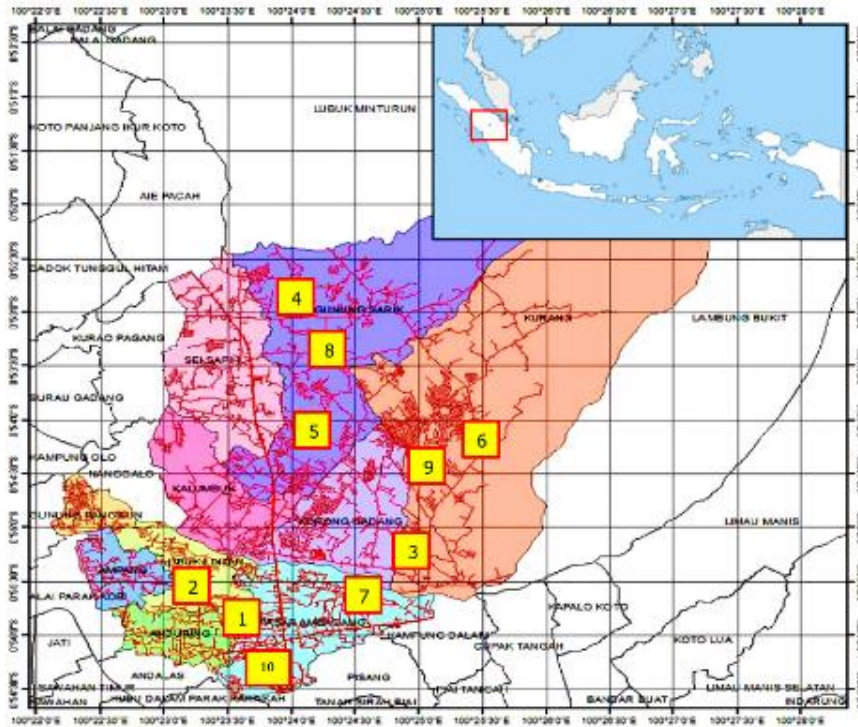


Figure 1: Location of infiltration measurements

The fifth stage is running the model using samples to obtain the infiltration rate and capacity. Infiltration capacity is determined using the Horton equation:

$$f = f_c + (f_0 - f_c) \cdot e^{-k \cdot t} \tag{1}$$

The *k* value (geophysical constant) is influenced by the soil conditions at each test location point, obtained using a linear equation.

$$k = \frac{-1}{0,434m} \tag{2}$$

The gradient value (*m*) is found using the formula $\log(f/f_c)$ cm/hour. Hereinafter, a graph is made with the x-axis : time and the y-axis : $\log(f/f_c)$. Based on the linear curve formed, the gradient value (*m*) is obtained from the graphic equation. The final stage is measuring the infiltration rate of the soil surface using a double ring infiltrometer as a comparison.

3. RESULTS

Infiltration measurements in residential land were carried out on the topsoil using a double ring infiltrometer, in average soil characteristic conditions: soil texture was clayey sand with water content (ω) of 31,6%,

soil bulk density (γ) of 1,73gr/cm³, porosity (*n*) of 33,98%, high soil density, soil permeability *K* of 0,0092 cm/jam, embankment thickness is 1meter, with a water content of 31.6%, soil bulk density γ is 1.73gr/cm³, porosity *n* is 33.98%, field soil density is dense, soil permeability *K* is 0.0092 cm/hour, embankment thickness is 1 meter, and the ratio of yard area to house building area is 15-20%.

3.1 Infiltration Capacity in Settlement Land

The calculation results for 10 measurement locations obtained an average constant infiltration rate (*f_c*) of 46,6mm/hour. This value is included in the medium category, meaning that when rain occurs, the water infiltration takes a long time, thus causing most of the rainwater will become surface runoff (Figure 2.a). Meanwhile, the average infiltration capacity calculated using the Horton equation was obtained at 59 mm/hour and the resulting curve is Figure 2.b.

3.2 Artificial Infiltration Model

The artificial infiltration model considers groundwater elevation, measurements of the average thickness of landfill in the plot, and the ratio of yard area to the house building area. The infiltration model is box-shaped with dimension of 50cm x 50cm x 100cm. This infiltration model was made using 10mm thick acrylic material, 60 x 60 x 3mm angle iron reinforcement, and 3mm thick strip iron (Figure 3).

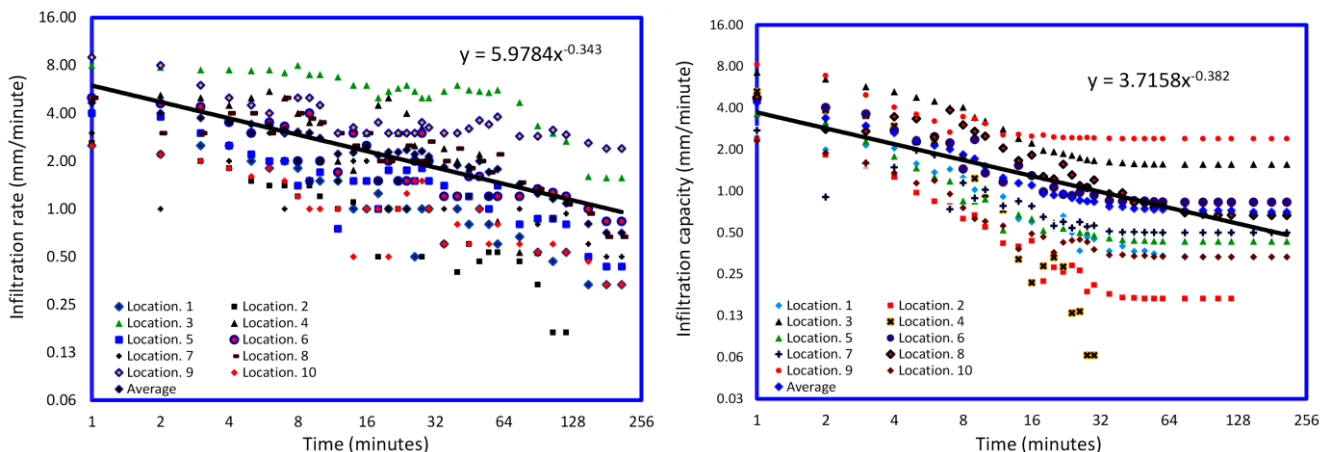


Figure 2: Infiltration rate and capacity curve in urban residential land

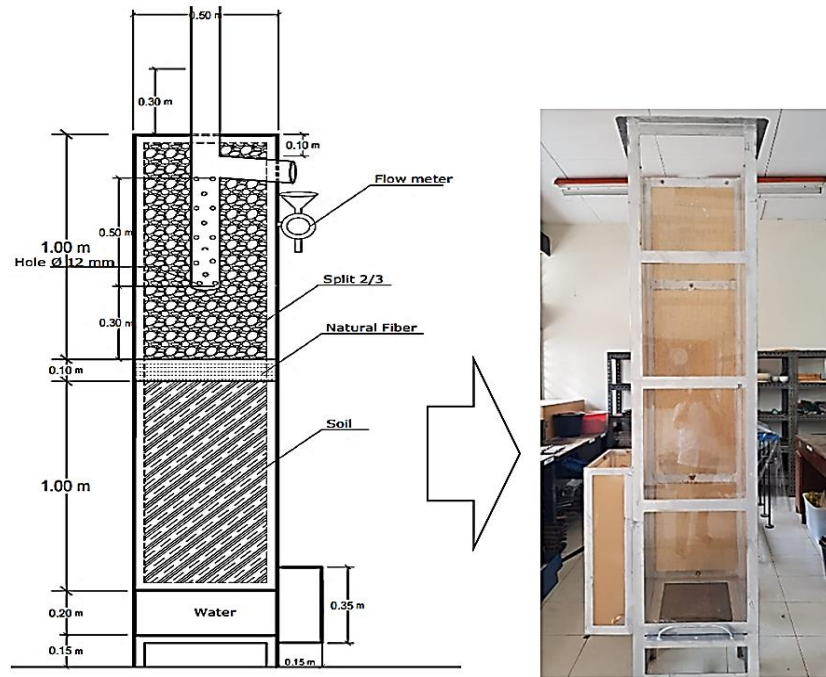


Figure 3: Design of the infiltration tool model

A layer of palm fiber 10 cm thick applied on the bottom to avoid sediment penetration due to uplift. In the middle of the box is installed vertically a 4 inch PVC pipe. The pipe has been pre-perforated with diameter of 12mm with a distance of 5cm between holes. The upper pipe section (10cm below ground surface level) is connected to a horizontal pipe of the same size. This horizontal pipe functions to remove excess water. The space between the pipe, box wall and fiber layer is filled 2 x 3cm apart to prevent water

from concentrating. Water flows through a $\frac{3}{4}$ inch pipe from the water tower to the top end of the vertical pipe. To keep the water flow from the tower constant, a flowmeter equipped with a tap is installed in the $\frac{3}{4}$ pipe. The excess water that comes out of the horizontal pipe is measured using a flowmeter. To maintain the stability of the tool so that uplift does not occur, the groundwater level is maintained at 1 meter below the surface of the soil sample (Figure 4).

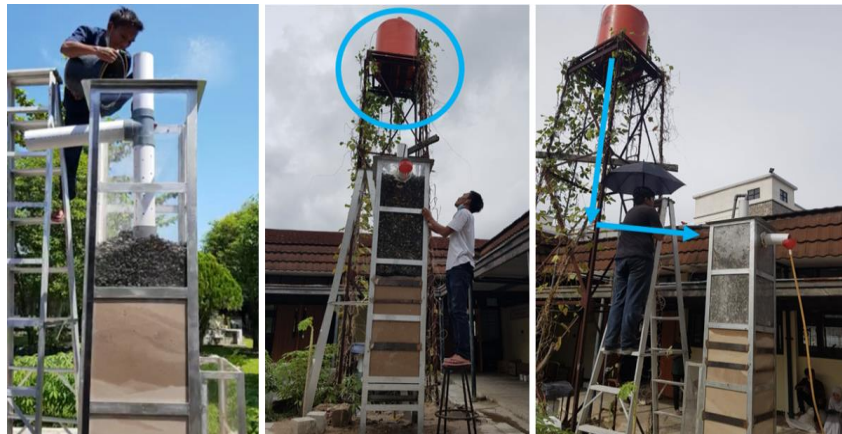


Figure 4: Installation of artificial infiltration model

3.3 Artificial Infiltration Models Performance

Test variations only include soil texture and water content. Meanwhile, the split absorption capacity constant at 3.1%, the soil bulk density constant at 1.31 gr/cm³, and the rain intensity constant at 84.8 mm/hour. Soil texture variations include loamy sand, sandy loam, and sand. Water content ranges from 39 – 41%.

The performance of the infiltration model starts from flowing water into the tank through a $\frac{3}{4}$ inch pipe equipped with a flowmeter flowing to a 4 inch pipe through the top end. The volume measured by the flowmeter is recorded every time interval Δt . If the speed of the incoming water exceeds the infiltration capacity of the tool, the remaining water will come out through the 4 inch pipe (outflow). The amount of water that comes out of the horizontal pipe is measured by a flowmeter installed on the horizontal pipe. The water that comes out of the model (outflow) is a surface flow parameter. If inflow \approx outflow then infiltration is considered constant and the test is stopped.

Infiltration volume is the volume of incoming water (inflow within a certain time period) minus the volume of outgoing water (outflow within a certain time period). Meanwhile, the height of the water drop (h) is the

infiltration volume (V) divided by the cross-sectional area of the infiltration model (A). The water height change (Δh) is the height of the water drop at each specified time interval. The infiltration rate is the water height change (Δh) divided by the time interval; $f = \Delta h / \Delta t$. The results of running the model are presented in Figure 5.a. The infiltration rate results obtained from running the new model are used as input to calculate infiltration capacity using the Horton equation. The calculation results for 5 quarry samples are presented in Figure 5.b

The infiltration rate curve (Figure 5.a) shows that the average constant infiltration rate (f_c) is 283.9mm/hour. This speed falls into the category of *very fast* according to the U.S. classification. Soil Conservation > 25.5 cm/hour (Kohnke, 1968). Infiltration capacity is determined by constant infiltration capacity (Ferré and Warrick, 2004). Based on the calculation results, it was found that the infiltration capacity in the Malintang Trench (PM) sample was 453.9mm/hour, Lubuk Alung (LA) was 435.6mm/hour, Lubuk Minturun (LM) was 250.4mm/hour, Sarik River (SS) was 370.6mm/hour, and the Gunung Sarik (GS) sample was 198.8mm/hour.

3.4 The Correlation of Rain, Infiltration and Surface Flow

The correlation between rainfall, infiltration and surface flow using an artificial infiltration model based on test results is presented in Figure 6.

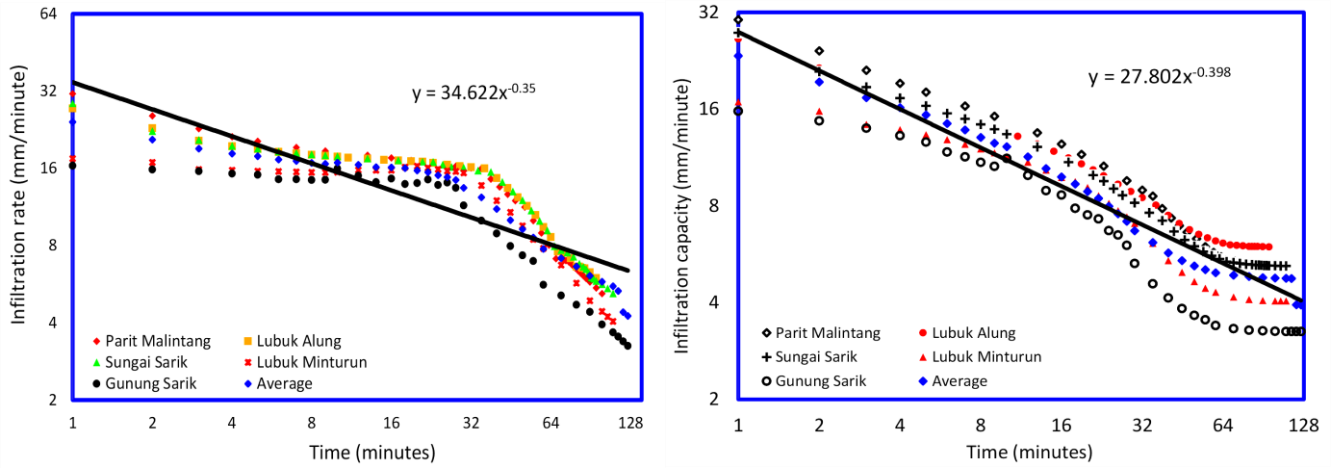


Figure 5: Infiltration rate of artificial infiltration model

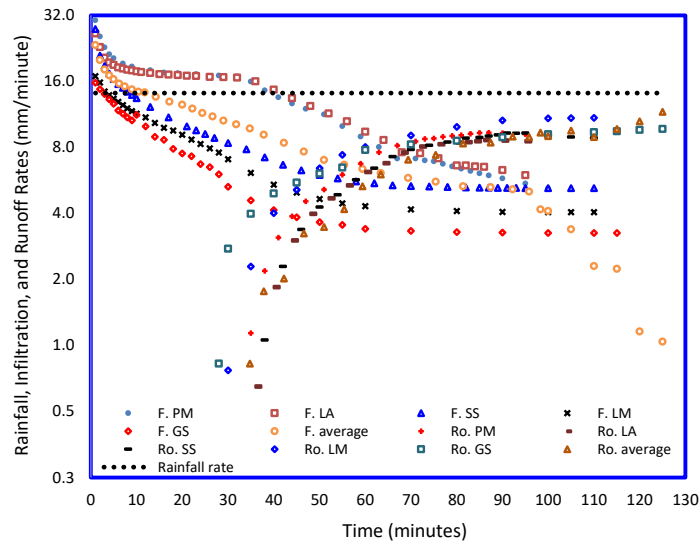


Figure 6: Infiltration, surface flow and rainfall intensity correlation from the average values in the artificial infiltration tool model.

The curve in Figure 6 can be simplified to see the relationship between infiltration, surface flow and rainfall intensity based on the results of all measurements on the artificial infiltration model (Figure 7).

From the curve in Figure 7, the equation for the average surface flow is $y=7.6382 \ln(x)-24.241$. The start of surface flow is calculated as follows:

$$y = 7,6382 \ln(x) - 24.241$$

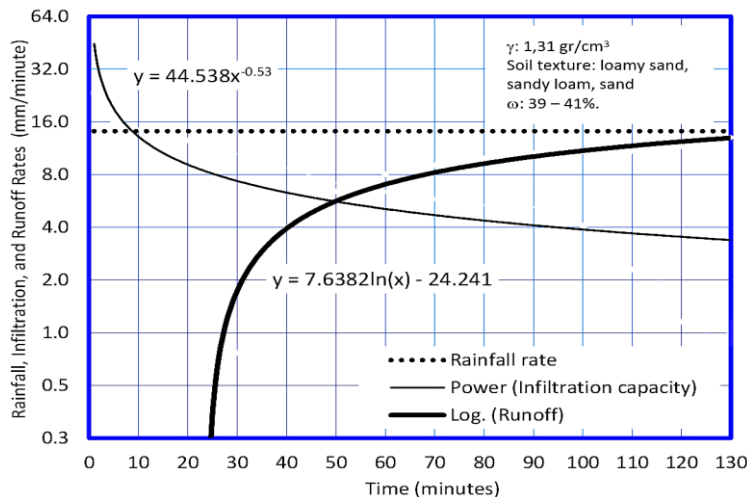
$$y + 24,241 = 7,6382 \ln(x)$$

$$\ln(x) = \frac{y + 24,241}{7,6382}$$

$$x = e^{\frac{y+24,241}{7,6382}}$$

At the initial time (y=0), then:

$$x = e^{\frac{y+24,241}{7,6382}} \approx 23,8 \text{ minutes}$$



Gambar 7: Correlation trends between infiltration, surface flow and rainfall intensity from the average values

4. DISCUSSION

The measurement results show that low infiltration in the surface layer of soil in urban residential areas is due to high levels of soil density, soil properties (water content and bulk density), soil texture, and fine soil fractions that clog the pores of the soil surface. This means that this soil layer is difficult for water to penetrate. To overcome this condition, a method or tool is needed that is able to pass water through the soil layer, to maintain high infiltration. One method is to create an artificial infiltration device. In this research, we have just created an artificial infiltration model.

The results of the infiltration capacity curve resulting from model testing show that the infiltration capacity at the start of the rain is the largest. When the soil becomes wet, it causes the infiltration capacity to decrease, then the infiltration capacity decreases with the length of time it rains until a constant infiltration value is reached. The calculation results of the arithmetic average infiltration capacity of all samples were 342mm/hour, while the soil surface infiltration capacity measured using a double ring infiltrometer was 59mm/hour. These results show that the new infiltration model is able to increase the infiltration capacity of the original soil 6 times. This means that this infiltration model can increase the absorption capacity of the soil up to 6 times.

The relationship between infiltration, rainfall and surface flow formed as the results of running the artificial infiltration model is in accordance with the theory stated by L. Rodney, et al and the results of several other studies related to infiltration, runoff and rainfall (Ferré and Warrick, 2004; Rodney et al., 2013).

The use of artificial infiltration models can slow down surface flow. The results of the calculation of the average surface flow occurred in the 23rd minute. If all settlements implement it in prototype form, then artificial infiltration has the potential to reduce flood peaks.

This artificial infiltration model also shifts the meeting point between the infiltration capacity curve and the average surface flow curve (critical point) at the 49th minute. In these conditions, surface flow is greater than the amount of water infiltrated, lead to increasing quantity of surface flow. By shifting this value, flooding can be reduced. Thus, this artificial infiltration model can increase infiltration capacity and reduce surface flow due to rainwater in urban residential areas

5. CONCLUSIONS

The infiltration model is a box measuring 50cm x 50cm with a depth of 100cm. The bottom of the box is given a layer of palm fiber 10cm thick, and installed a 4 inches PVC pipe in the middle which has been perforated with a hole diameter of 12 mm with a distance of 5 cm between hole and installed vertically, respectively. The top end of the pipe is connected to a 4 inches horizontal pipe which is connected to the urban drainage system. The space between the pipe, the box wall and the palm fiber layer is filled by 2x3cm split.

The calculation results of the arithmetic average infiltration capacity using the artificial infiltration model were 342 mm/hour, while the infiltration capacity at the ground surface was only 59 mm/hour. These results show that the new infiltration model is able to increase the infiltration capacity of the original soil by up to 6 times.

The relationship between rainfall, infiltration and surface flow using an artificial infiltration model is in accordance with existing theory, so that this artificial infiltration model has the potential to reduce surface rainwater flow and can reduce peak flood discharge by increasing infiltration capacity.

ACKNOWLEDGEMENTS

The author would like to express his gratitude to Mas Mera, Junaidi, and Dalrino for their guidance and discussions. Author is also thank Rusli HAR for assistance with data collection in the field.

REFERENCES

Alaoui, A., Rogger, M., Peth, S., and Blöschl, G., 2018. Does soil compaction increase floods? A review. *Journal of Hydrology*, 557, December, Pp. 631–642. <https://doi.org/10.1016/j.jhydrol.2017.12.052>

Andayono, T., 2018. The Effect of Soil Density on Infiltration Rate in The Urban Development Area of Padang. *Jurnal Teknik Sipil and Perencanaan*, 20(1), Pp. 1–5. <https://doi.org/10.1016/j.jhydrol.2017.12.052>

doi.org/10.15294/jtsp.v20i1.12387

Arvand, S., Ganji Noroozi, Z., Delghandi, M., and Alipour, A., 2023. Evaluating the impact of LID-BMPs on urban runoff reduction in an urban sub-catchment. *Urban Water Journal*, Pp. 1–12. <https://doi.org/10.1080/1573062X.2023.2207083>

Basset, C., Abou Najm, M., Ghezzehei, T., Hao, X., and Daccache, A., 2023. How does soil structure affect water infiltration? A meta-data systematic review. *Soil and Tillage Research*, 226, October 2022. <https://doi.org/10.1016/j.still.2022.105577>

Bean, E. Z., and Dukes, M. D., 2015. Effect of amendment type and incorporation depth on runoff from compacted sandy soils. *Journal of Irrigation and Drainage Engineering*, 141(6), Pp. 1–12. <https://doi.org/10.1061/ASCE,IR.1943-4774.0000840>

Fahim Aslam, M., Habib-ur-Rehman, M., and Muhammad Khan, N., 2021. Assessing the Role of Infiltration Galleries to Enhance Groundwater Recharge in Model Town Lahore. *American Journal of Water Science and Engineering*, 7(1), 14. <https://doi.org/10.11648/j.ajwse.20210701.12>

Ferré, T. P. A., and Warrick, A. W., 2004. Infiltration. *Encyclopedia of Soils in the Environment*, 4, 1977, Pp. 254–260. <https://doi.org/10.1016/B0-12-348530-4/00382-9>

Jennings, A. A., and Baker, K., 2016. Hydraulic Performance of a Residential Stormwater Infiltration Gallery. *Journal of Environmental Engineering, United States*, 142(3), Pp. 1–9. <https://doi.org/10.1061/ASCE.EE.1943-7870.0001063>

Kirenda, V., and Mugume, S. N., 2019. Effectiveness of infiltration galleries in reduction of surface runoff and flooding in urban areas. *Novatech*, July, Pp. 1–6.

Kodikara, J., Islam, T., and Sountharajah, A., 2018. Review of soil compaction: History and recent developments. *Transportation Geotechnics*, 17, September, Pp. 24–34 <https://doi.org/10.1016/j.trgeo.2018.09.006>

Kohnke, H., 1968. *Soil physics*. New York : McGraw-Hill Companies.

Kuma, H. G., Feyessa, F. F., and Demissie, T. A., 2023. Assessing the impacts of land use / land cover changes on hydrological processes in Southern Ethiopia : The SWAT model approach Assessing the impacts of land use /land cover changes on hydrological processes in Southern Ethiopia: The SWAT model approach. *Cogent Engineering*, 10(1). <https://doi.org/10.1080/23311916.2023.2199508>

Locatelli, L., Mark, O., Mikkelsen, P. S., Arnbjerg-Nielsen, K., Deletic, A., Roldin, M., and Binning, P. J., 2017. Hydrologic impact of urbanization with extensive stormwater infiltration. *Journal of Hydrology*, 544, Pp. 524–537. <https://doi.org/10.1016/j.jhydrol.2016.11.030>

Meng, X., Li, X., Nghiem, L. D., Ruiz, E., Johir, M. A., Gao, L., and Wang, Q., 2022. Improved stormwater management through the combination of the conventional water sensitive urban design and stormwater pipeline network. *Process Safety and Environmental Protection*, 159, Pp. 1164–1173. <https://doi.org/10.1016/j.psep.2022.02.003>

Mgolozeli, S., Ncizah, A. D., Wakindiki, I. I. C., Mudau, F. N., and Onwona-Agyeman, S., 2022. Investigation of Infiltration and Runoff Rate on Agri-Mats Using a Laboratory Rainfall Simulation Study. *Communications in Soil Science and Plant Analysis*, 54(8), Pp. 1005–1014. <https://doi.org/10.1080/00103624.2022.2137187>

Molla, E., Getnet, K., and Mekonnen, M., 2022. Land use change and its effect on selected soil properties in the northwest highlands of Ethiopia. *Heliyon*, 8(8), e10157. <https://doi.org/10.1016/j.heliyon.2022.e10157>

Obour, P. B., and Ugarte, C. M., 2021. A meta-analysis of the impact of traffic-induced compaction on soil physical properties and grain yield. *Soil and Tillage Research*, 211, August 2020, Pp. 105019. <https://doi.org/10.1016/j.still.2021.105019>

Rodney, L., Fangmeier, D. D., and Elliot, W. J., 2013. Infiltration and Runoff. In *Soil and Water Conservation Engineering Seventh Edition*, Seventh ed, Pp. 81–113. <https://doi.org/10.13031/swce.2013.5>

- Shahzad, H., Myers, B., Boland, J., Hewa, G., and Johnson, T., 2022. Stormwater runoff reduction benefits of distributed curbside infiltration devices in an urban catchment. *Water Research*, 215, 118273. <https://doi.org/10.1016/j.watres.2022.118273>
- Wu, W., Jamali, B., Zhang, K., Marshall, L., and Deletic, A., 2023. Water Sensitive Urban Design, WSUD. Spatial Prioritisation through Global Sensitivity Analysis for Effective Urban Pluvial Flood Mitigation. *Water Research*, 235, 119888. <https://doi.org/10.1016/j.watres.2023.119888>
- Xiao, F., Wang, X., and Fu, C., 2023. Impacts of land use/land cover and climate change on hydrological cycle in the Xiaoxingkai Lake Basin. *Journal of Hydrology: Regional Studies*, 47, December 2022, Pp. 101422. <https://doi.org/10.1016/j.ejrh.2023.101422>
- Yu, M., Mapuskar, S., Lavonen, E., Oskarsson, A., McCleaf, P., and Lundqvist, J., 2022. Artificial infiltration in drinking water production: Addressing chemical hazards using effect-based methods. *Water Research*, 221, Pp. 118776. <https://doi.org/10.1016/j.watres.2022.118776>
- Zaout, T., Andradóttir, H. Ó., and Arnalds, Ó., 2022. Infiltration capacity in urban areas undergoing frequent snow and freeze-thaw cycles: Implications on sustainable urban drainage systems. *Journal of Hydrology*, Pp. 607. <https://doi.org/10.1016/j.jhydrol.2022.127495>

